7th International Conference on Debris-Flow Hazards Mitigation

Looking through the window of disturbance at post-wildfire debris-flow hazards

Luke A. McGuire[a,*], Francis K. Rengers[b], Jason W. Kean[b], Dennis M. Staley[b], Hui Tang[a], Ann M. Youberg[c]

[a]University of Arizona, Department of Geosciences, 1040 E 4th St, Tucson, AZ 85721, USA
[b]U.S. Geological Survey, 1711 Illinois St., Golden, CO 80401, USA
[c]University of Arizona, Arizona Geological Survey, 1955 E 6th St., Tucson, AZ 85721, USA

Abstract

The extreme heat from wildfire alters soil properties and incinerates vegetation, leading to changes in infiltration capacity, ground cover, soil erodibility, and rainfall interception. These changes promote increases in runoff and sediment transport that increase the likelihood of runoff-generated debris flows. Over a period of several years, referred to as the window of disturbance, the landscape recovers and wildfire-induced changes become less accentuated. Debris flows are most common in the year immediately following wildfire, but changes in the likelihood and magnitude of debris flows throughout the window of disturbance are not well constrained. Assessing debris-flow hazards throughout the post-wildfire recovery period is complicated, in part, by the myriad of wildfire-induced changes and their nonlinear relationships with sediment transport and runoff generation processes. In this study, we combine measurements of soil hydraulic properties with vegetation survey data and numerical modeling to understand how debris-flow threats are likely to change in steep, burned basins during the first two years of recovery. We focus on documenting recovery following the 2016 Fish Fire in the San Gabriel Mountains, CA, USA and demonstrate how a numerical model can be used to predict temporal changes in debris-flow properties and initiation thresholds within that region. Substantial increases in sorptivity, which represents the capillarity contribution to infiltration, and reductions in the percentage of bare soil occurred during the first 18 months following the Fish Fire. Numerical modeling suggests that these changes lead to a roughly 40% increase in the 15-minute rainfall intensity-duration threshold associated with debris-flow initiation as well as more than a three-fold decrease in debris-flow volume from post-fire year 1 to post-fire year 2. These results provide valuable constraints on changes in debris-flow thresholds within the San Gabriel Mountains as well as a general framework for exploring the impact of changing vegetation and soil hydraulic properties on debris flow magnitude and susceptibility.

Keywords: debris flow, wildfire, recovery, threshold, infiltration

1. Introduction

Wildfire is a well-documented catalyst for change in hydrologic and geomorphic systems (e.g. Shakesby and Doerr, 2006). Post-wildfire reductions in infiltration capacity (Ebel and Moody, 2017) and canopy interception (Stoof et al., 2012) promote increased runoff. Increased runoff combined with the effects of lower critical thresholds for sediment entrainment (Moody et al., 2005) and a high percentage of bare soil lead to a substantial increase in debris-flow likelihood after a wildfire. Post-wildfire debris flows are triggered when runoff concentrates in steep channels and mobilizes large volumes of sediment, in contrast to debris flows that initiate from shallow landslides (e.g. Meyer and Wells, 1997; Cannon et al., 2008; Gabet and Bookter, 2008; Kean et al., 2011). With few exceptions (e.g. Cannon et al., 2008), previous work has focused on the threats posed by runoff-generated debris flows in the first year following disturbance by wildfire, but the extent to which debris flow hazards persist into subsequent years is not well understood.

Rainfall intensity-duration (ID) thresholds are commonly used to assess post-wildfire debris-flow potential, with debris flows often initiating once a critical rainfall intensity is exceeded (Cannon et al., 2008; Staley et al., 2013).

* Corresponding author e-mail address*: lmcguire@email.arizona.edu*

Staley et al. (2017) recently developed an empirical model to predict debris-flow likelihood as a function of terrain attributes, soil burn severity, and rainfall intensity (averaged over 15, 30, or 60 minutes). However, it is not clear how rainfall ID thresholds change with time following wildfire because data regarding debris-flow occurrence are most common in the first post-wildfire year and because there is no clear connection between the magnitude of empirically

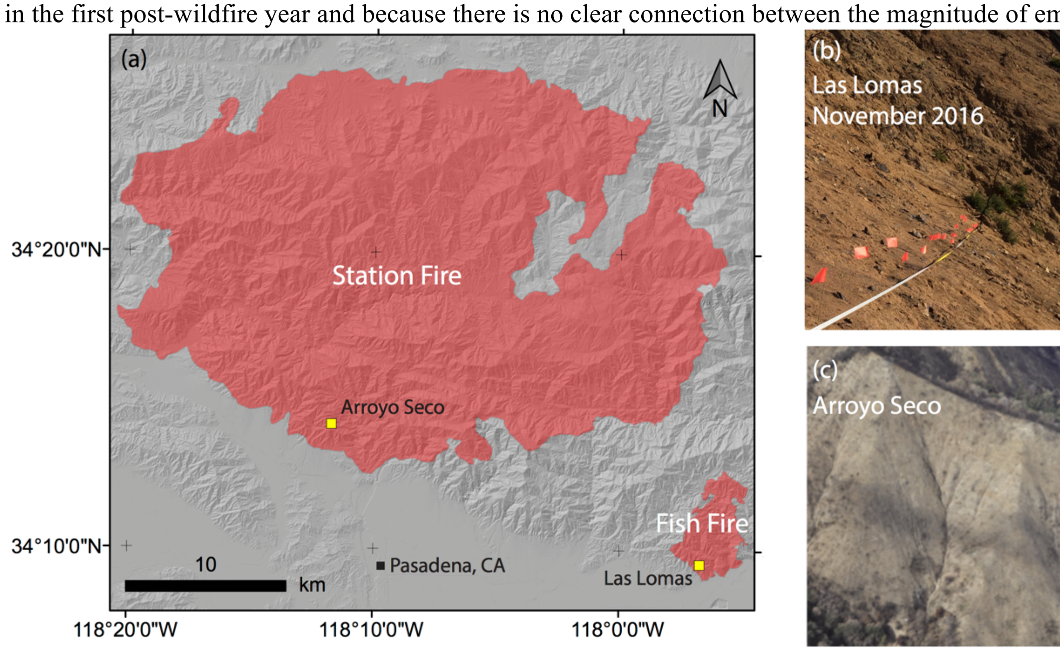

Fig. 1. (a) Overview of study area; (b) Photo looking across the hillslope along a transect at the Las Lomas site where infiltration measurements were conducted. (c) Aerial photo of the Arroyo Seco watershed following the 2009 Station Fire.

derived rainfall ID thresholds and the hydrologic and geomorphic variables that are changing as the landscape recovers. Since runoff is a necessary condition for most post-wildfire debris flows, it is critical to understand how wildfire-driven changes to soil infiltration capacity change with time since burning and how the magnitude of those changes translates into changes in debris-flow potential. Post-wildfire reductions in infiltration capacity are often attributed to increased soil water repellency (Shakesby and Doerr, 2006), which may persist for up to five years but typically decays over timescales of 1-2 years (e.g. Larsen et al., 2009). The percentage of bare soil, which is initially high following wildfire and decays as vegetation recovers, is also likely to be a key factor in determining debris-flow potential since bare soil on hillslopes is particularly vulnerable to erosion. Hillslope erosion can account for a substantial amount of the sediment within post-wildfire debris flows in certain cases (e.g. Smith et al., 2012; Staley et al., 2014) and contribute to sediment bulking in the channel that increases flow depth and discharge.

Given measurements of how wildfire-affected variables change over time, such as ground cover and soil hydraulic properties, physically-based models have the potential to be used to quantify the corresponding changes in debris-flow response. In this study, we utilize the numerical model developed by McGuire et al. (2017), which represents the coupled processes of runoff, sediment transport, and debris-flow initiation, to assess changes in debris-flow ID thresholds and debris-flow magnitude within an 18-month period following wildfire in the San Gabriel Mountains, CA, USA. We make use of data from two study areas, referred to as Las Lomas and Arroyo Seco, both of which are located in the San Gabriel Mountains and have produced numerous debris flows following wildfire. Although the two study sites were burned at different times and in different fires (Figure 1), we utilize them as representative sites for debris-flow prone headwater basins in the San Gabriel Mountains. Data from the Las Lomas study site are used to quantify changes in soil hydraulic properties and canopy/ground cover with time following wildfire. Changes in soil hydraulic properties were quantified at Las Lomas through in situ measurements throughout an 18-month period following the 2016 Fish Fire. Canopy and ground cover were negligible at the start of the study period and were quantified through a field survey 18 months after the Fish Fire. These measurements are then used as inputs for a numerical model in conjunction with a high resolution digital elevation model (DEM), obtained at the nearby Arroyo Seco site (which was the focus of intensive debris-flow monitoring following the 2009 Station Fire), to simulate debris-flow initiation during different stages of recovery. Here, we report on the measured changes at Las Lomas and a series of simulations designed to assess how debris-flow response is likely to change in the San Gabriel Mountains from the first to second year after the wildfire.

2. Study Area

The Fish Fire, which started on 21 June 2016, burned 4253 acres of the Angeles National Forest in the San Gabriel Mountains near Los Angeles, CA (Figure 1). The wildfire burned mainly in rugged terrain with steep hillslopes dominated by chaparral vegetation. Soils in the area are generally thin (0.5-1 m), rock outcrops are common, and a highly weathered layer of saprolite is occasionally exposed on the hillslopes (Staley et al., 2014). Repeat measurements of soil hydraulic properties were conducted on a roughly 40-degree hillslope, which we will refer to as the Las Lomas study site, in an area that experienced moderate-to-high soil burn severity during the Fish Fire. No vegetation canopy remained and all litter and duff at the surface had been consumed by the wildfire. The hillslope is located in the upper portion of a 0.12 km^2 basin that drains into the Las Lomas debris basin. A series of rainstorms between December 2016 and February 2017 incised a network of rills through the study area and produced a number of debris flows and floods at the outlet of the drainage basin.

The Arroyo Seco site, also located in the San Gabriel Mountains in an area dominated by chaparral vegetation, is a small drainage basin (0.012 km^2) that burned at moderate-to-high severity in the 2009 Station Fire. A number of runoff-generated debris flows were observed in the first winter following the fire (Kean et al., 2011). A DEM derived from terrestrial laser scanner (TLS) surveys performed by Staley et al. (2014) following the first post-wildfire rainstorms provides high-resolution topographic data that are ideal for detailed simulations of runoff and debris flow initiation.

3. Methods

3.1. Field measurements following the Fish Fire

Field saturated hydraulic conductivity (K_s) and sorptivity (S) were determined through in situ measurements conducted with a mini disk tension infiltrometer. The tension infiltrometer has a disk with a radius of 2.25 cm. The suction head was set to 1 cm for all measurements. Measurements were made during site visits to the Las Lomas study area (burned in the 2016 Fish Fire) in September 2016, November 2016, January 2017, February 2017, July 2017, and March 2018. Measurements were performed every 1 meter along a 20 meter transect that extended in the cross-slope direction, with the exception of those made in September 2016. When time permitted, additional measurements were made on the hillslope in the vicinity of the established transect. In September 2016, the transect had not yet been established and measurements were made in nearby areas burned at moderate-high severity.

A total of 26, 35, 28, 40, 21, and 21 infiltration measurements were made during the site visits in September 2016, November 2016, January 2017, February 2017, July 2017, and March 2018, respectively. During each measurement, the total volume of water infiltrated is tracked as a function of time and must later be post-processed to infer field saturated hydraulic conductivity (K_s) and sorptivity (S) (e.g. Zhang, 1997). Estimates of K_s and S were derived using the methods described by McGuire et al. (2018). The wetting front suction head (h_f), a parameter in the Green-Ampt infiltration model, can then be estimated as (Ebel and Moody, 2016) $h_f = S^2/2K_s\theta_s$, where θ_s denotes the volumetric water content at saturation.

In March 2018, we conducted a vegetation survey on a hillslope adjacent to the infiltration transect using the point-intercept method (e.g. Crocker and Tiver, 1948). A measuring tape was extended between two control points marked with steel rebar. The distance between the two control points was 20.8 meters. Every 20 cm along the transect (for a total of 105 measurements), we sighted directly down toward the surface with a laser pointer and recorded the first obstacle that intercepted the light. The laser either hit the vegetation canopy, bare soil, litter, or a rock. Litter was classified as any loose plant material on the soil surface. Any sediment with a diameter greater than 5 mm was classified as rock cover. If the laser hit any portion the canopy, the maximum height of that vegetation was recorded.

3.2. Numerical model

The numerical model represents fluid flow using the shallow water equations, which contain additional source terms to account for changes in flow resistance as a function of sediment concentration (McGuire et al., 2016; 2017). Infiltration is modeled with the Green-Ampt equation, using estimates of K_s and h_f obtained from field measurements. Hydraulic roughness was taken into account using a depth-dependent Manning friction coefficient (Mugler et al., 2011). Debris-flow resistance is represented using a Coulomb friction approach (e.g. Iverson and Denlinger, 2001) where the effective basal normal stress is modified by pore fluid pressure within the flow. In all simulations, the ratio of pore fluid pressure to total basal normal stress (λ) was set to a constant value of λ=0.65.

The Hairsine-Rose (HR) model (Hairsine and Rose, 1992a; 1992b) was used to account for sediment entrainment and deposition, as described in detail by McGuire et al. (2016). In the HR model, particles can be detached and entrained into the flow via raindrop impact or flow-driven detachment. The rate at which sediment is detached by raindrops is a function of flow depth, rainfall intensity, and raindrop diameter while the rate of flow-driven sediment detachment is a function of stream power. Since the canopy and ground cover (e.g. litter) can shield the underlying soil from raindrop impact, changes in ground and canopy cover will also influence the rate of raindrop-driven sediment detachment (e.g. McGuire et al., 2016).

3.3. Debris-flow simulations at Arroyo Seco

For model simulations, we applied the vegetation and hydrologic measurements from the Fish Fire to the nearby Arroyo Seco drainage basin (Figure 1) because a high-resolution DEM was available for that site. Although Arroyo Seco was not burned during the Fish Fire, it is representative of headwater areas within the San Gabriel Mountains where post-wildfire debris flows tend to initiate and its steepness is similar to other debris-flow producing basins in the San Gabriel Mountains (Kean et al., 2011). The small size of the basin makes it possible to perform a larger number of simulations, and we coarsened the DEM from 2 cm (Staley et al., 2014) to a grid spacing of 37.5 cm to further increase computational efficiency. Runoff is driven by a family of idealized rainstorms, with peak 15-minute rainfall intensities (I_{15}) varying from 20 mm/h to 60 mm/h in increments of 2.5 mm/h (Figure 2).

All simulations were performed using the same parameters and model setup as reported in McGuire et al. (2016) unless otherwise noted (Table 1). McGuire et al. (2016) calibrated the HR sediment transport parameters at the Arroyo Seco site by comparing simulated erosion patterns to those generated from repeat TLS surveys (Staley et al., 2014). The roughness coefficient was set to a value of n_0=0.05 s m$^{-1/3}$, which is in range of calibrated roughness values for recently burned, low-order drainage basins in the San Gabriel Mountains (Rengers et al., 2016). The fraction of bare soil exposed to raindrop impact is assumed to be 1.0 in the first year following the fire based on field observations of negligible vegetation and litter cover (Figure 1). Infiltration rates were computed for year 1 using the K_s and h_f values obtained in September 2016 and November 2016, while K_s and h_f values obtained in July 2017 and March 2018 were used for year 2. Each pixel within the computational domain was randomly assigned a value from the measured distribution of K_s and h_f. Due to the number of pixels in the computational domain, we found that differences among simulations performed with different realizations of K_s and h_f were not significant.

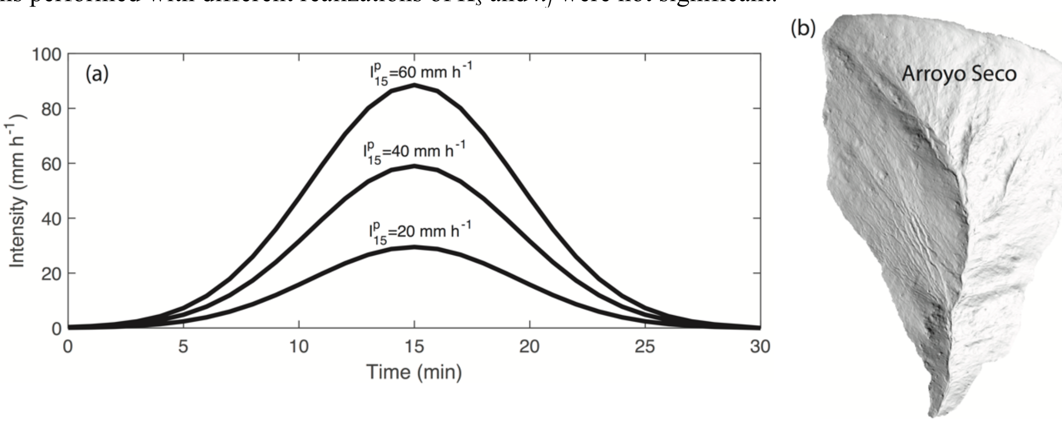

Fig. 2. (a) Designed rainstorms used for simulations at Arroyo Seco. For display purposes only 3 curves are shown; however, for modeling we used curves with peak 15-minute rainfall intensity (I_{15}^p) varying from 20-60 mm h^{-1} in intervals of 2.5 mm h^{-1}; (b) Shaded relief map of Arroyo Seco.

A total of 19 simulations, each driven by one of the 19 different rainstorms (Figure 2a), were performed using the measured infiltration and vegetation characteristics from the first post-wildfire year. A second set of 19 simulations were performed using the measured infiltration and vegetation characteristics from the second post-wildfire year. Lastly, we performed a final set of simulations using measured soil hydraulic properties from year 2 and vegetation characteristics (i.e. 100% bare ground) consistent with year 1. The goal of these simulations was to quantify the relative impact of vegetation recovery and soil recovery on post-wildfire debris flows. Flow depth, discharge, and sediment concentration at the basin outlet were recorded in all cases to assess differences among simulations. Debris flows were identified at the outlet of the basin based on exceedance of a sediment concentration threshold of 40%. Flows with a sediment concentration (*c*) less than 40% were classified as floods. The total volume of sediment exiting the basin, total volume of debris flows (i.e. flows with c>40%) leaving the basin, and peak debris flow discharge at the outlet were stored for each simulation.

Table 1. Model parameters used for simulations of runoff, sediment transport, and debris flow initiation at the Arroyo Seco site. Notation follows McGuire et al. (2016). When appropriate, values for year 1 and year 2 are both presented and separated by commas. Median values are reported for K_s and h_f.

Parameter name (symbol)	Units	Value	Source
Roughness coefficient (n_0)	s m$^{-1/3}$	0.05	Calibrated
Raindrop detachability (a_0)	kg m^{-2} s^{-1}	9000	Calibrated
Raindrop redetachability (a_{d0})	kg m^{-2} s^{-1}	410000	Calibrated
Fraction of effective stream power (F)	-	0.0065	Calibrated
Fraction canopy cover	-	0, 0.29	Measured
Fraction bare soil	-	1, 0.63	Measured
Field saturated hydraulic conductivity (K_s)	mm h^{-1}	17, 13	Measured
Wetting front suction head (h_f)	m	0.005, 0.022	Measured

4. Results

4.1. Changes in soil hydraulic properties and ground cover

Repeat field measurements of soil hydraulic properties reveal a change in sorptivity (S) between February 2017 and July 2017, which corresponds to a time period of 8 to 13 months after the wildfire (Figure 3). As a result, the median wetting front suction head (h_f) increased with time from roughly 0.001 m in September 2016 to 0.021 m by March 2018. In contrast, field saturated hydraulic conductivity (K_s) appears to be relatively constant with time following the wildfire (Figure 3). The first and third quartiles of K_s in year 1 are 9 mm/h and 33 mm/h, respectively, whereas they are 5 mm/h and 30 mm/h in year 2. The fraction of bare soil decreased from 1.0 immediately following the wildfire to 0.63 in March 2018, after 18 months of recovery. The reduction in bare ground was primarily due to an increase in canopy cover fraction from approximately 0 to 0.29. The fractions of litter (0.07) and rock cover (0.01) were relatively minor. Although the recovering vegetation may be effective at reducing direct raindrop impact on the soil surface, it likely had a minimal ability to intercept and store water since the average vegetation height was less than 10 cm.

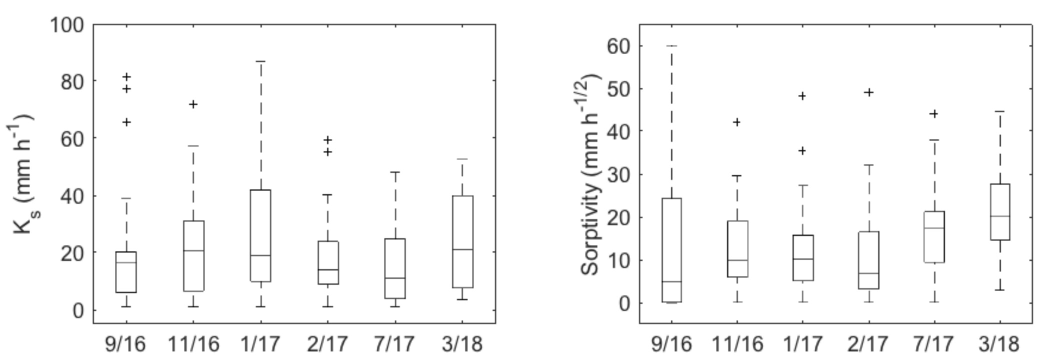

Fig. 3. (a) Field saturated hydraulic conductivity (K_s) and (b) sorptivity (*S)* derived from field measurements at different times following the June 2016 Fish Fire.

4.2. Simulations of erosion and debris flows

Debris flows initiated in response to lower intensity rainstorms in year 1 relative to year 2 (Figure 4). The first sign of debris flow activity at the lower outlet (i.e. debris flow volume greater than 5 m^3) during year 1 occurs in response to the designed rainstorm with a peak I_{15} of 27.5 mm/h whereas storms during year 2 with a peak I_{15} less than 37.5 mm/h do not produce any debris flows at the outlet. In the theoretical case where vegetation recovery is neglected in year 2 and only changes in infiltration capacity are taken into account, a peak I_{15} of at least 35 mm/h is required to initiate debris flows.

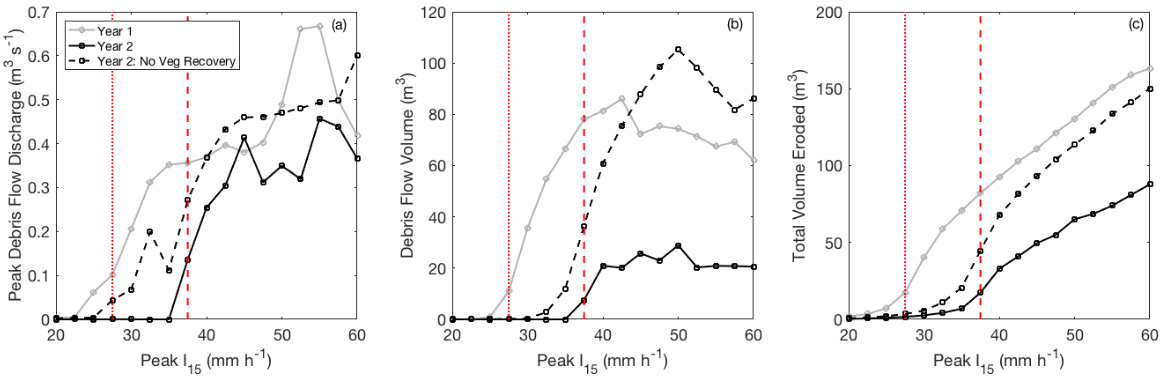

Fig. 4. Model simulations of (a) debris-flow discharge, (b) debris-flow volume, and (c) total volume eroded at the basin outlet as a function of rainfall intensity. Vertical lines indicate model-derived thresholds for year 1 (dotted line) and year 2 (dashed line). (a) Peak debris flow discharge and (c) total sediment volume eroded generally increase with peak I_{15} and are highest in the first year following the fire. (b) Debris flow volumes are limited at higher rainfall intensities due to the increased amount of water runoff, which can reduce sediment concentrations in the flow.

The peak discharge of debris flows generally increases with peak I_{15} and decreases from year 1 to year 2, though peak flow depths (Figure 5) and discharges (Figure 4a) are sometimes comparable between years 1 and 2. Debris-flow volume initially increases with peak I_{15} and then remains constant (year 2) or decreases slightly (year 1). The total volume of sediment eroded, however, continues to increase with peak I_{15}. Debris flow-volumes and total sediment eroded for a given rainstorm are higher in year 1, as expected, with the exception of the case where the site experiences high-intensity rainfall and vegetation recovery is neglected during year 2 simulations.

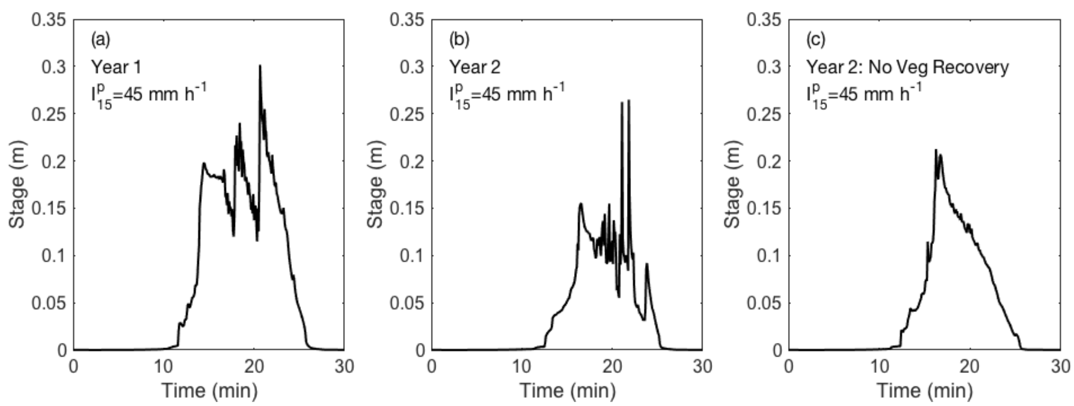

Fig. 5. Model simulations of flow stage at the Arroyo Seco basin outlet under conditions consistent with (a) post-wildfire year 1, (b) post-wildfire year 2, and (c) post-wildfire year 2 where we assume that the vegetation did not recover (i.e. canopy and litter cover are negligible).

5. Discussion

Simulations of erosion and debris-flow initiation suggest that there should be a substantial increase in rainfall ID thresholds between the first and second year after a wildfire as well as decreases in expected debris flow volume due to changes in soil hydraulic properties. Simulations do not take into account the reductions in sediment supply that are likely to have occurred in the time between the first and second year after a wildfire. Results reported here can therefore be viewed as conservative, with even greater increases in ID thresholds and reductions in volume being likely if sediment supply is reduced in subsequent years from erosion occurring during year 1.

Thresholds of 27.5 mm/h and 37.5 mm/h can be inferred from simulations for years 1 and 2, respectively. The regional I_{15} threshold for debris flow initiation in the San Gabriel Mountains is 19 mm/h (Staley et al., 2013). The difference between the regional threshold and the value derived here could result from basin-specific morphological properties that influence debris flow thresholds (e.g. Staley et al., 2017), uncertainties associated with measured soil hydraulic properties, or from the choice of the designed rainstorm. Increases in the threshold rainfall intensity from 27.5 mm/h in year 1 to 37.5 mm/h year 2 can be attributed to both the increase in h_f and a decrease in percent bare ground. Increases in h_f lead directly to decreases in runoff. Low values of sorptivity (and therefore h_f) in the year immediately following wildfire are consistent with a recent compilation of soil hydraulic properties from burned soils (Ebel and Moody, 2017), which suggests that sorptivity rather than K_s may be more consistently affected by wildfire. Decreases in percent bare ground lead to less hillslope erosion, which subsequently decreases the amount of sediment transported into the channel network (where debris flows are likely to form) and reduces the sediment bulking processes that can increase flow depths and discharges. However, since simulations that neglect vegetation recovery still suggest a 7.5 mm/h increase in the 15-minute rainfall ID threshold, we conclude that changes in infiltration capacity have a greater impact on temporal variations in the rainfall ID threshold relative to changes in percent bare ground.

Simulations also offer insight into how debris flow magnitude can be expected to change with rainfall intensity and time since burning. Simulations indicate that debris-flow volume increases, up to a point, with increasing I_{15} (Figure 4). Gartner et al. (2014), in contrast, found that debris-flow volumes increase monotonically with I_{15} based on a large dataset of estimated volumes from post-wildfire debris flows throughout the Transverse Ranges of southern CA. The difference between our model results and field observations could be partly due to the definition of debris flow employed here, which requires that the sediment concentration exceed 40%. As I_{15} increases, the modeled erosion volumes increase monotonically but debris-flow volumes remain steady or decrease due to increased water runoff, which can dilute portions of the flow to sediment concentrations less than 40%. Since debris flow volumes estimated in the field are based on the amount of sediment deposited in debris basins or estimates of erosion occurring during debris-flow-producing rainstorms (e.g. Gartner et al., 2014), they may include sediment transported through a combination of water-dominated flood, debris flood, and debris-flow mechanisms. Regardless, it is clear that debris flow volumes appear to change more dramatically (i.e. a factor of roughly 3) between year 1 and year 2 compared to the I_{15} rainfall threshold (Figure 4), which increases by approximately 40%. Note that the high debris-flow volumes simulated in year 2 during a case with no vegetation recovery likely exceed those predicted for year 1 due to the fact that increased water runoff in year 1 will dilute some of the flows so that they have a concentration less than the critical value of 40%.

While we focus on a particular geographic region, the San Gabriel Mountains in southern CA, the modeling framework presented here can be used in combination with estimates of post-wildfire infiltration rates from other regions (e.g. Moody et al., 2009; Nyman et al., 2011; Robichaud et al., 2016) to quantify the impact of changing soil hydraulic properties on debris-flow magnitude and initiation thresholds. Similarly, satellite-derived metrics of vegetation recovery, such as the enhanced vegetation index (e.g. Kinoshita and Hogue, 2011), could be used to drive temporal changes in percent ground cover within the model framework. Developing relationships between measurable hydrologic variables, ground cover characteristics, and debris flow properties is a necessary first step towards assessing how debris flow threats are likely to evolve with time following wildfire in different geographic regions.

Conclusions

Disturbance following wildfire leads to an increased potential for runoff-generated debris flows. The hazards posed by debris flows decrease with time following wildfire as soils and vegetation recover. In this study, we monitored changes in soil hydraulic properties and percent bare ground at a site in southern California and used a numerical model to determine how temporal changes in these two variables affect debris flow volumes and initiation thresholds. Simulations suggest that the threshold I_{15} rainfall intensity that triggers debris flows at our study site in the San Gabriel Mountains will increase by approximately 40%, from 27.5 mm/h to 37.5 m/h. In addition, if debris flows do initiate in the second post-wildfire year, simulations indicate they will be roughly three times smaller (even if sediment supply does not decrease between year 1 and year 2). Although we focus here on post-wildfire debris flows, the methodology used to assess changes in runoff-generated debris flow susceptibility could be applied in other settings, including rocky alpine regions, where runoff-generated debris flows may occur.

Acknowledgements

We would like to thank Petter Nyman and Joe Gartner for thoughtful reviews that improved the quality of this manuscript. This work was supported by the U.S. Geological Survey (USGS) Landslide Hazards Program. Any use of trade, product, or firm names is for descriptive purposes only and does not imply endorsement by the U.S. Government. Code for the numerical model used in this study is available through the Community Surface Dynamics Modeling System (CSDMS) model repository.

References

Cannon, S.H., Gartner, J.E., Wilson, R.C., Bowers, J.C. and Laber, J.L., 2008, Storm rainfall conditions for floods and debris flows from recently burned areas in southwestern Colorado and southern California: Geomorphology, v. 96, no. 3-4, 250-269.

Crocker, R.L. and Tiver, N.S., 1948, Survey methods in grassland ecology: Grass and Forage Science, v. 3, no. 1, 1-26.

Iverson, R.M. and Denlinger, R.P., 2001, Flow of variably fluidized granular masses across three-dimensional terrain: 1. Coulomb mixture theory. Journal of Geophysical Research: Solid Earth, v. 106 (B1), 537-552.

Ebel, B.A. and Moody, J.A., 2017, Synthesis of soil-hydraulic properties and infiltration timescales in wildfire-affected soils: Hydrological processes, v. 31, no. 2, 324-340.

Gabet, E.J. and Bookter, A., 2008, A morphometric analysis of gullies scoured by post-fire progressively bulked debris flows in southwest Montana, USA.: Geomorphology, v. 96, no. 3-4, 298-309.

Gartner, J.E., Cannon, S.H. and Santi, P.M., 2014, Empirical models for predicting volumes of sediment deposited by debris flows and sediment-laden floods in the transverse ranges of southern California: Engineering Geology, v. 176, 45-56.

Hairsine, P.B. and Rose, C.W., 1992a, Modeling water erosion due to overland flow using physical principles: 1. Sheet flow: Water resources research, v. 2, no. 1, 237-243.

Hairsine, P.B. and Rose, C.W., 1992b, Modeling water erosion due to overland flow using physical principles: 2. Rill flow: Water resources research, v. 28, no. 1, 245-250.

Kean, J.W., Staley, D.M., and Cannon, S.H., 2011, In situ measurements of post- fire debris flows in southern California: Comparisons of the timing and magnitude of 24 debris-flow events with rainfall and soil moisture conditions: Journal of Geophysical Research, v. 116, F04019, 10.1029/2011JF002005.

Kinoshita, A.M. and Hogue, T.S., 2011, Spatial and temporal controls on post-fire hydrologic recovery in Southern California watersheds: Catena, v. 87, no. 2, 240-252.

Larsen, I.J., MacDonald, L.H., Brown, E., Rough, D., Welsh, M.J., Pietraszek, J.H., Libohova, Z., de Dios Benavides-Solorio, J. and Schaffrath, K., 2009, Causes of post-fire runoff and erosion: water repellency, cover, or soil sealing?: Soil Science Society of America Journal, v. 73, no. 4, 1393-1407.

Meyer, G.A. and Wells, S.G., 1997, Fire-related sedimentation events on alluvial fans, Yellowstone National Park, USA: Journal of Sedimentary Research, v. 67, no. 5, 776-791.

McGuire, L.A., Kean, J.W., Staley, D.M., Rengers, F.K., and Wasklewicz, T.A., 2016, Constraining the relative importance of raindrop- and flow-driven sediment transport mechanisms in post-wildfire environments and implications for recovery time scales: Journal of Geophysical Research: Earth Surface, 10.1002/2016JF003867

McGuire, L.A., Rengers, F.K., Kean, J.W. and Staley, D.M., 2017, Debris flow initiation by runoff in a recently burned basin: Is grain- by- grain sediment bulking or en masse failure to blame?: Geophysical Research Letters, v. 44, no. 14, 7310-7319.

McGuire, L.A., Rengers, F.K., J Kean, J.W., Staley, D.M. and Mirus, B.B., 2018, Incorporating spatially heterogeneous infiltration capacity into hydrologic models with applications for simulating post-wildfire debris flow initiation: Hydrological Processes, 10.1002/hyp.11458.

Moody, J.A., Smith, J.D. and Ragan, B.W., 2005, Critical shear stress for erosion of cohesive soils subjected to temperatures typical of wildfires: Journal of Geophysical Research: Earth Surface, v. 110, F1.

Moody, J.A., Kinner, D.A. and Úbeda, X., 2009, Linking hydraulic properties of fire-affected soils to infiltration and water repellency: Journal of Hydrology, v. 379, no. 3-4, 291-303.

Mügler, C., Planchon, O., Patin, J., Weill, S., Silvera, N., Richard, P. and Mouche, E., 2011, Comparison of roughness models to simulate overland flow and tracer transport experiments under simulated rainfall at plot scale: Journal of Hydrology, v. 402, no. 1-2, 25-40.

Nyman, P., Sheridan, G.J., Smith, H.G., and Lane, P.N., 2011, Evidence of debris flow occurrence after wildfire in upland catchments of south-east Australia: Geomorphology, v. 125, no. 3, 383-401. 2000.

Rengers, F.K., McGuire, L.A., Kean, J.W., Staley, D.M., and Hobley, D., 2016, Model simulations of flood and debris flow timing in steep catchments after wildfire: Water Resources Research, v. 52, 6041–6061, doi:10.1002/2015WR018176.

Robichaud, P.R., Wagenbrenner, J.W., Pierson, F.B., Spaeth, K.E., Ashmun, L.E. and Moffet, C.A., 2016, Infiltration and interrill erosion rates after a wildfire in western Montana, USA: Catena, v. 142, 77-88.

Shakesby, R.A. and Doerr, S.H., 2006. Wildfire as a hydrological and geomorphological agent, Earth-Science Reviews, v. 74, no. 3-4, 269-307.

Smith, H.G., Sheridan, G.J., Nyman, P., Child, D.P., Lane, P.N., Hotchkis, M.A. and Jacobsen, G.E., 2012, Quantifying sources of fine sediment supplied to post-fire debris flows using fallout radionuclide tracers: Geomorphology, v. 139, 403-415.

Staley D.M., Kean, J.W., Cannon, S.H., Laber, J.L., and Schmidt, K.M., 2013, Objective definition of rainfall intensity-duration thresholds for the initiation of post-fire debris flows in southern California: Landslides, v. 10, 547-562. doi:10.1007/s10346-012-0341-9

Staley, D.M., Wasklewicz, T.A. and Kean, J.W., 2014, Characterizing the primary material sources and dominant erosional processes for post-fire debris-flow initiation in a headwater basin using multi-temporal terrestrial laser scanning data: Geomorphology, v. 214, 324-338.

Staley, D.M., Negri, J.A., Kean, J.W., Laber, J.L., Tillery, A.C., and Youberg, A.M., 2017, Prediction of spatially explicit rainfall intensity–duration thresholds for post-fire debris-flow generation in the western United States: Geomorphology, v. 278, 149-162

Stoof, C.R., Vervoort, R.W., Iwema, J., Elsen, E., Ferreira, A.J.D. and Ritsema, C.J., 2012, Hydrological response of a small catchment burned by experimental fire: Hydrology and Earth System Sciences, v. 16, no. 2, 267-285.

Zhang, R., 1997, Determination of soil sorptivity and hydraulic conductivity from the disk infiltrometer: Soil Science Society of America Journal, v. 61, no. 4, 1024-1030.